

Approaching the Chiral and Continuum Limit of Large- N QCD

Evan Wickenden^{a,*} and Thomas DeGrand^a

^a*Department of Physics, University of Colorado,
Boulder, CO 80309, USA*

E-mail: evan.wickenden@colorado.edu, thomas.degrand@colorado.edu

We present preliminary results from our calculation of the low energy constants (LECs) of the chiral effective theory for 3, 4 and 5 color QCD with $N_f = 2$ dynamical fermion flavors. We simulate with clover fermions over a range of lattice couplings and quark masses. We observe the expected N_c scaling for the LECs appropriate to the condensate B and pseudoscalar decay constant F . The range of quark masses over which leading order chiral perturbation theory describes the data grows as N_c rises.

*The 38th International Symposium on Lattice Field Theory, LATTICE2021 26th-30th July, 2021
Zoom/Gather@Massachusetts Institute of Technology*

*Speaker

1. Introduction

The large N_c limit provides interesting insight into nonperturbative features of QCD [1–3]. The lattice offers a means to test its predictions. The objective of our study is to simulate across N_c with $N_f = 2$ flavors of dynamical fermions, measure the low energy constants (LECs) of chiral perturbation theory (χ PT), and observe their N_c scaling. We aim to extrapolate our results to $a \rightarrow 0$ and $N_c \rightarrow \infty$.

The results shown here are preliminary. We observe the expected N_c scaling for the leading LECs: $B \sim N_c^0$ and $F \sim N_c^{1/2}$. A feature we observe is that the region of parameter space where χ PT describes the data is larger at larger N_c . This is due to the fact that the chiral expansion may be written in terms of the parameter $\xi = \frac{m_\pi^2}{8\pi^2 f_\pi^2}$, which, because $f_\pi^2 \sim N_c$, is naturally suppressed at large N_c .

A large N_c study with $N_f = 2$ flavors in the chiral and continuum limit is absent from the literature. A number of other approaches to the large N_c limit have been studied. Hernandez et al. considered the $N_f = 4$ case with 3 – 6 colors at a single lattice spacing [4]. Bali et al. studied spectroscopy with 2-7 and 17 colors in the quenched approximation [5]. Using Eguchi-Kawai reduction, according to which finite-volume effects vanish as $N_c \rightarrow \infty$, Gonzalez-Arroyo and collaborators have performed studies at extremely large N_c [6]. Our goal is to make comparisons with these and other studies.

2. Wilson Chiral Perturbation Theory

χ PT has a set of LECs which characterize the quark mass dependence of quantities such as m_π^2 , f_π . Predictions for these observables through NNLO are present in the literature. They are typically presented using two different expansions: the x and ξ expansions, where

$$x \equiv \frac{2Bm_q}{4\pi^2 F^2}, \quad \xi \equiv \frac{m_\pi^2}{4\pi f_\pi^2} \quad (1)$$

Using ξ rather than x amounts to a resummation of the chiral expansion. Careful studies in the SU(3) case with $N_f = 2(+1)$ fermions demonstrate that the ξ expansion has better convergence properties, with the NNLO formulae describing lattice data to larger fermion or pseudoscalar masses [7–9]. A theoretical justification for this behavior is that the NNLO chiral logs in the ξ expansion have smaller numerical coefficients than they do in the x expansion. Following these results, we work primarily with the ξ expansion. We plan to do fits with the x expansion as a consistency check.

QCD on the lattice has chiral symmetry explicitly broken by both nonzero quark mass and nonzero lattice spacing. Wilson Chiral Perturbation Theory ($W\chi$ PT) enhances chiral perturbation theory at the level of the effective Lagrangian by introducing operators with an explicit dependence on lattice spacing. These operators arise from the Symanzik action for QCD via a spurion analysis. Using the power counting scheme $\delta \sim p^2 \sim m_q \sim a$, Bar, Rupak and Shoresh derive the effective chiral Lagrangian for Wilson-type fermions through $\mathcal{O}(\delta^2)$ [10]. The NLO $W\chi$ PT predictions for

m_π^2/m_q and f_π are:

$$\begin{aligned}\frac{m_\pi^2}{m_q} &= 2B\left(1 + \frac{1}{2}\xi \log \xi\right) + L_M \xi + W_q a + \tilde{W}_{qq} \frac{a^2}{\xi} \\ f_\pi &= F(1 - \xi \log \xi) + L_f \xi + W_F a.\end{aligned}\tag{2}$$

The W 's are the correction terms due to the use of Wilson fermions.

We use the Wilson flow parameter t_0 to set the scale. t_0 depends on the bare parameters in the simulation, and thus on measured observables. The dependence of the gradient flow scale t_0 on m_{PS}^2 was described by Bar and Golterman [11]. Using a t_0 which is mass-dependent (as was done by Ref. [12]) does not alter the chiral logarithms, but it does affect the L_i 's in Eq. 2. We need a mass-independent definition of a lattice spacing, which we obtain by interpolating $m_\pi^2 \sqrt{t_0}$ versus t_0 to 0.15 for our data at a given β .

We match scales across N_c in the commonly - used way, taking

$$t_0^2 \langle E(t_0) \rangle = C(N_c)\tag{3}$$

with

$$C(N_c) = C \left(\frac{3 N_c^2 - 1}{8 N_c} \right),\tag{4}$$

and $C = 0.3$ the usual value used in $SU(3)$. Our data span a range of $t_0 = 1$ to 3 or so, corresponding (with an $SU(3)$ value of $\sqrt{t_0} \sim 0.15$ fm) to $a = 0.09 - 0.15$ fm.

3. Simulation and Analysis Methodology

We use the HMC algorithm with the Wilson gauge action with nHYP links and clover fermions [13]. We have mostly simulated on $16^3 \times 32$ lattices, with a few $24^3 \times 32$ volumes used as cross checks. For each data point, we collected between 400 and several thousand trajectories, keeping every 10th configuration for measurements. A jackknife analysis is used to obtain errors on and correlations between lattice observables. By increasing the number of deletions and monitoring how the errors grow, we can roughly estimate how autocorrelated the data are, and find them to be minimally so. We discard at least the first hundred trajectories for thermalization, and further test for thermalization by walking out the minimum trajectory and watching for drifting observables. Most of the data points included in our analysis have $m_\pi L > 4$; a few are slightly below this threshold. The Python package `gvar` is used to automatically track errors and correlations, alongside `lsqfit` for correlated nonlinear least squares fitting [14, 15].

Pion masses, decay constants and Axial Ward Identity quark masses are all determined in the usual way of fitting correlators to hyperbolic functions. As a way to reduce systematic errors associated with choosing fit ranges, we employ Neil and Jay's Bayesian model-averaging method [16]. This weights each fit proportionally to $e^{-\chi^2/2+N}$, where N is the number of points included in the fit, which balances a small chi-squared against a larger fit range.

4. Chiral Fits

In Fig. 1 we present plots of $m_\pi^2 \sqrt{t_0}/m_q$ and $f_\pi \sqrt{t_0}$ versus ξ for 3, 4, and 5 colors. We fit these to standard NLO χ PT at each lattice spacing (i.e. neglecting the Wilson terms), and in Fig. 2 plot the a -dependence we obtain in B , F , L_M , and L_F .

5. Analysis

The plots for F and L_F show small a dependence and appear to extrapolate to a common value of $\sqrt{t_0} \sqrt{3/N_c} F \sim 0.07 - 0.08$ or $\sqrt{3/N_c} F \sim 90 - 100$ MeV (recall we are working in a convention where $f_\pi \sim 131$ MeV), or $\sqrt{3/N_c} F \sim 60 - 70$ MeV in the “93 MeV” f_π convention. This is a reasonable number, according to the tables in Ref. [7]. $\sqrt{t_0} B$ has larger a -dependence, but a value of $\sqrt{t_0} B \sim 2.0 - 2.4$ gives $\Sigma^{1/3} \sim 250$ MeV, again not an unreasonable value.

The above plots also convey a novel feature of this project: the chiral limit becomes easier at larger N_c , in that a constant range of ξ corresponds to a much wider range of m_q . Again, this is simply due to the fact that $\xi \sim m_\pi^2/f_\pi^2 \sim m_q/N_c$. This is nevertheless very useful, since it means that at larger N_c , one can obtain good chiral data while staying further away from the computational challenges of very light dynamical quarks. ξ also governs the size of finite volume effects, so these are also reduced at larger N_c . In Fig. 2, one can see the LECs are much better determined for 5 colors than 4 or 3 (and they appear to have less lattice spacing dependence), despite arising from fewer net trajectories. At three colors, on a $16^3 \times 32$ lattice, we are squeezed between finite volume effects and keeping ξ small enough for good fits to NLO chiral formulae. In fact, the bottleneck to our project is $N_c = 3$, which is of course much less interesting than $N_c > 3$ due to the availability of much better data by other collaborations. We only need it to cross check our results. For this reason we have found it necessary to begin running on $24^3 \times 32$ lattices.

6. Conclusion

In this project we aim to make continuum predictions for the low energy constants of chiral perturbation theory with $N_f = 2$ dynamical fermions. We aim to assess how well large N_c predictions describe the physical SU(3) case and to compare our results with other approaches to the large N_c limit, namely studies with different fermion content—different N_f ’s and/or different representations.

We have so far only used the next-to-leading order prediction of SU(N_f) Wilson chiral perturbation theory, with the standard power counting scheme $\delta \sim p^2 \sim m_q \sim a$. In the large N_c limit, the axial anomaly vanishes and the η meson recovers its status as a Goldstone boson, so $U(N_f)$ χ PT becomes the correct low-energy description of QCD. Considering alternative power counting schemes, NNLO predictions, and $U(N_f)$ χ PT are directions for future study.

Data collection and analysis continue. The goal remains first SU(2) \times SU(2) fits at each N_c , then global U(2) \times U(2) fits incorporating all data across N_c .

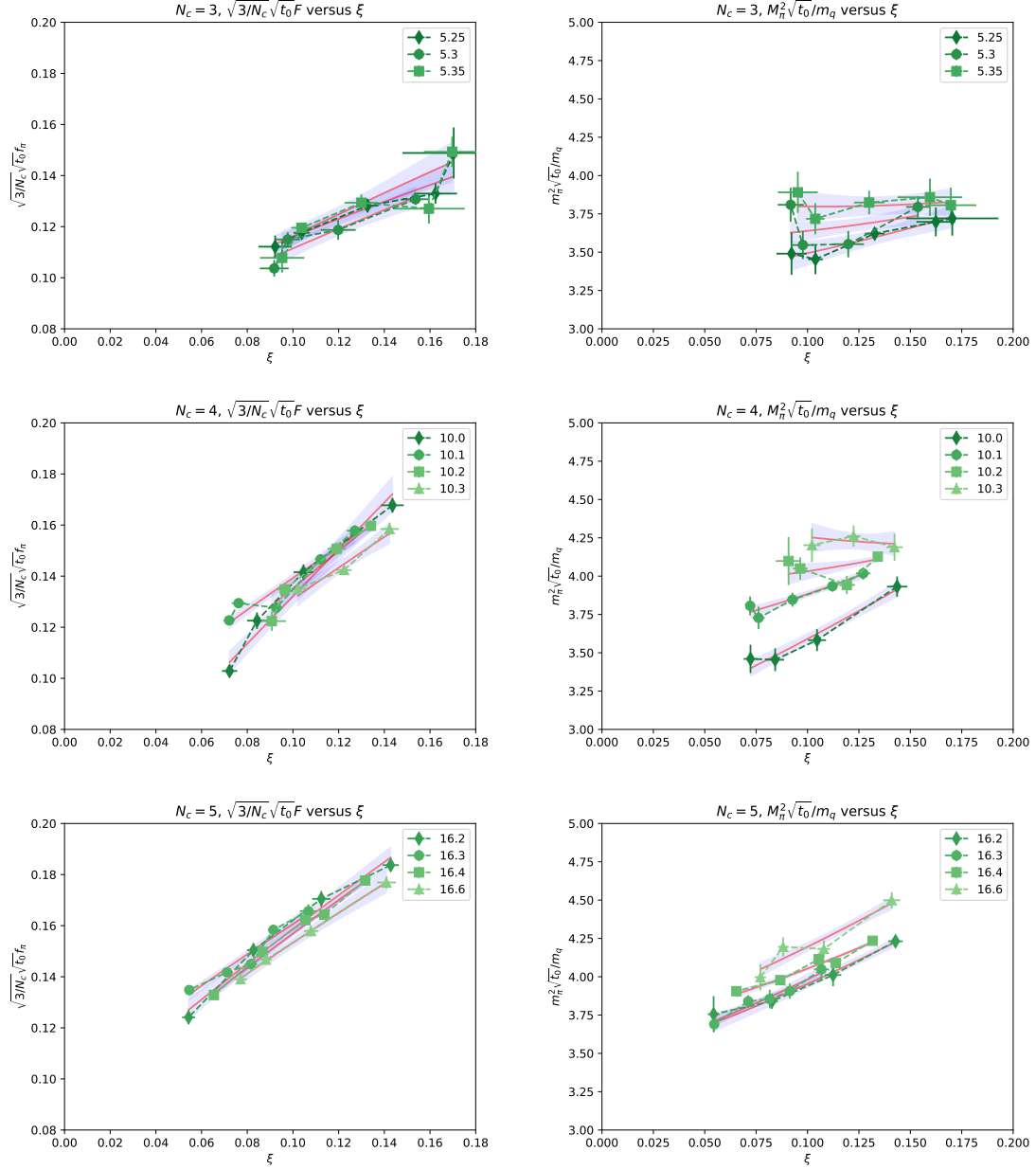


Figure 1: Left: pion decay constant scaled by $\sqrt{t_0} \sqrt{3/N_c}$ for 3,4,5 colors. Right: squared pion mass divided by AWI quark mass (again scaled by $\sqrt{t_0}$). The lines and colored bands show the results of NLO χ PT fits to the individual β values, neglecting the W_i 's in Eq. 2.

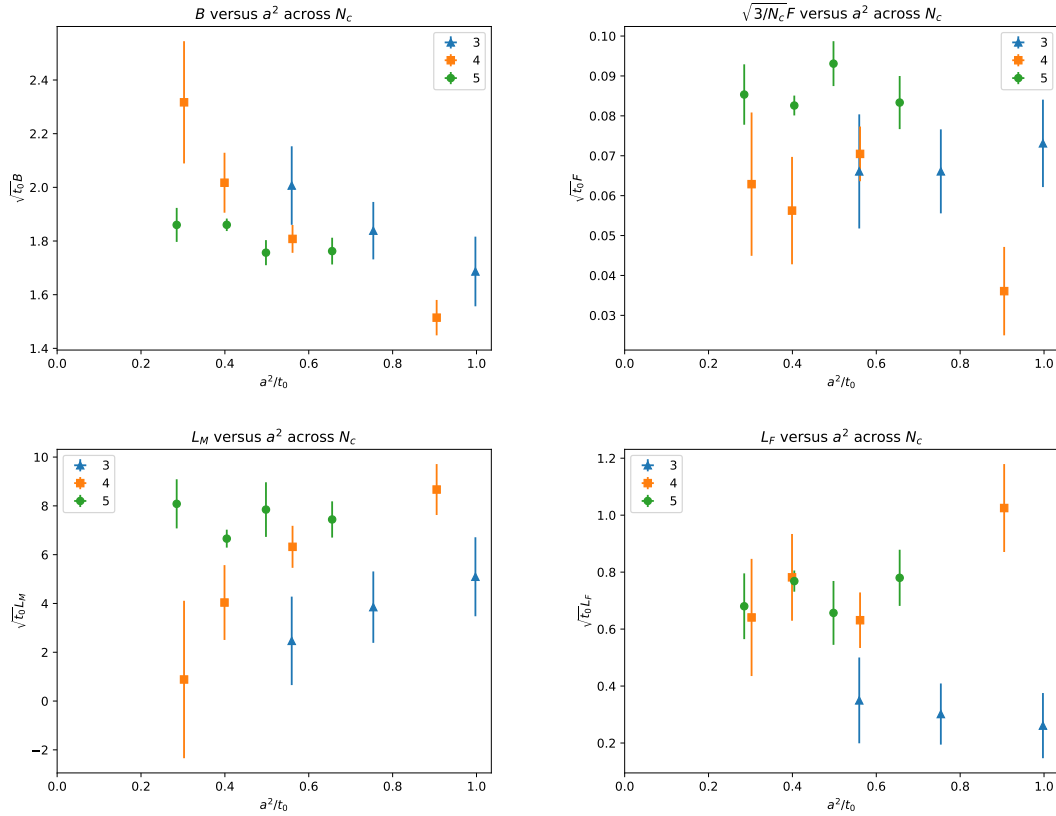


Figure 2: Preliminary plots of B , F , L_M , L_F (all in units of $\sqrt{t_0}$) versus a^2/t_0 . F is scaled by $\sqrt{3/N_c}$. Blue points are SU(3), orange points SU(4), green points SU(5).

Acknowledgments

This material is based upon work supported by the U.S. Department of Energy, Office of Science, Office of High Energy Physics under Award Number DE-SC-0010005. Some of the computations for this work were also carried out with resources provided by the USQCD Collaboration, which is funded by the Office of Science of the U.S. Department of Energy using the resources of the Fermi National Accelerator Laboratory (Fermilab), a U.S. Department of Energy, Office of Science, HEP User Facility. Fermilab is managed by Fermi Research Alliance, LLC (FRA), acting under Contract No. DE-AC02-07CH11359. Our computer code is based on the publicly available package of the MILC collaboration [17]. The version we use was originally developed by Y. Shamir and B. Svetitsky.

References

- [1] G. 't Hooft, Nucl. Phys. B **72**, 461 (1974) doi:10.1016/0550-3213(74)90154-0
- [2] G. 't Hooft, Nucl. Phys. B **75**, 461 (1974). doi:10.1016/0550-3213(74)90088-1

- [3] E. Witten, *Annals Phys.* **128**, 363 (1980) doi:10.1016/0003-4916(80)90325-5
- [4] P. Hernández, C. Pena and F. Romero-López, *Eur. Phys. J. C* **79**, no.10, 865 (2019) doi:10.1140/epjc/s10052-019-7395-y [arXiv:1907.11511 [hep-lat]].
- [5] G. S. Bali, F. Bursa, L. Castagnini, S. Collins, L. Del Debbio, B. Lucini and M. Panero, *JHEP* **1306**, 071 (2013) doi:10.1007/JHEP06(2013)071 [arXiv:1304.4437 [hep-lat]].
- [6] M. G. Pérez, A. González-Arroyo and M. Okawa, *JHEP* **04**, 230 (2021) doi:10.1007/JHEP04(2021)230 [arXiv:2011.13061 [hep-lat]].
- [7] S. Aoki *et al.* [Flavour Lattice Averaging Group], *Eur. Phys. J. C* **80**, no.2, 113 (2020) doi:10.1140/epjc/s10052-019-7354-7 [arXiv:1902.08191 [hep-lat]].
- [8] J. Noaki *et al.* [JLQCD and TWQCD], *Phys. Rev. Lett.* **101**, 202004 (2008) doi:10.1103/PhysRevLett.101.202004 [arXiv:0806.0894 [hep-lat]].
- [9] S. Dürr *et al.* [Budapest-Marseille-Wuppertal], *Phys. Rev. D* **90**, no.11, 114504 (2014) doi:10.1103/PhysRevD.90.114504 [arXiv:1310.3626 [hep-lat]].
- [10] O. Bar, G. Rupak and N. Shores, *Phys. Rev. D* **70**, 034508 (2004) doi:10.1103/PhysRevD.70.034508 [arXiv:hep-lat/0306021 [hep-lat]].
- [11] O. Bar and M. Golterman, *Phys. Rev. D* **89**, no.3, 034505 (2014) [erratum: *Phys. Rev. D* **89**, no.9, 099905 (2014)] doi:10.1103/PhysRevD.89.034505 [arXiv:1312.4999 [hep-lat]].
- [12] V. Ayyar, T. DeGrand, M. Golterman, D. C. Hackett, W. I. Jay, E. T. Neil, Y. Shamir and B. Svetitsky, *Phys. Rev. D* **97**, no.7, 074505 (2018) doi:10.1103/PhysRevD.97.074505 [arXiv:1710.00806 [hep-lat]].
- [13] A. Hasenfratz and F. Knechtli, *Phys. Rev. D* **64**, 034504 (2001) doi:10.1103/PhysRevD.64.034504 [arXiv:hep-lat/0103029 [hep-lat]].
- [14] P. Lepage, C. Gohlke, & D. Hackett, (2021). gplepage/gvar: gvar version 11.9.4 (v11.9.4). Zenodo. <https://doi.org/10.5281/zenodo.5479009>
- [15] P. Lepage, C. Gohlke. (2021). gplepage/lqfit: lqfit version 12.0.1 (v12.0.1). Zenodo. <https://doi.org/10.5281/zenodo.5512582>
- [16] W. I. Jay and E. T. Neil, *Phys. Rev. D* **103**, 114502 (2021) doi:10.1103/PhysRevD.103.114502 [arXiv:2008.01069 [stat.ME]].
- [17] https://github.com/milc-qcd/milc_qcd/